JPET Fast Forward. Published on July 12, 2010 as DOI: 10.1124/jpet.110.167551

Diminished activity-dependent BDNF expression underlies cortical neuron microcircuit hypoconnectivity resulting from exposure to mutant huntingtin fragments

Luca Gambazzi, Ozgun Gokce, Tamara Seredenina, Elena Katsyuba, Heike Runne, Henry Markram, Michele Giugliano and Ruth Luthi-Carter

Laboratory of Neural Microcircuitry, Brain Mind Institute, Ecole Polytechnique Fédérale de Lausanne (EPFL), Lausanne, Switzerland (LG, HM)

Laboratory of Functional Neurogenomics, Brain Mind Institute, Ecole Polytechnique Fédérale de Lausanne (EPFL), Lausanne, Switzerland (OG, TS, EK, HR, RLC)

Dept. of Biomedical Sciences, University of Antwerp, Wilrijk, Belgium (MG)

Running title: Cortical microcircuits and BDNF in Huntington's disease

Corresponding author:

Ruth Luthi-Carter, EPFL SV BMI LNGF, Station 15, CH-1015 Lausanne

ruth.luthi-carter@epfl.ch, tel: +41 21 693 6533, fax: + 41 21 693 9628

Number of text pages: 39

Number of tables: 1

Number of figures: 5

Number of references: 44

Number of words in *Abstract*: 240

Number of words in *Introduction*: 427

Number of words in *Discussion*: 1481

Non standard abbreviations: Population burst (PB), Inter burst interval (IBI), Multi Electrode Array (MEA), Spike-time histograms (STH)

Section assignment: Neuropharmacology

JPET Fast Forward. Published on July 12, 2010 as DOI: 10.1124/jpet.110.167551
This article has not been copyedited and formatted. The final version may differ from this version.

Abstract

Although previous studies of Huntington's disease (HD) have addressed many potential mechanisms of striatal neuron dysfunction and death, it is also known based on clinical findings that cortical function is dramatically disrupted in HD. With respect to disease etiology, however, the specific molecular and neuronal circuit bases for the cortical effects of mutant huntingtin (htt) have remained largely unknown. In the present work we studied the relation between the molecular effects of mutant htt fragments in cortical cells and the corresponding behavior of cortical neuron microcircuits using a novel cellular model of HD. We observed that a transcript-selective diminution in activity-dependent BDNF expression preceded the onset of a synaptic connectivity deficit in *ex vivo* cortical networks, which manifested as decreased spontaneous collective burst-firing behavior measured by multi-electrode array substrates. Decreased BDNF expression was determined to be a significant contributor to network-level dysfunction, as shown by the ability of exogenous BDNF to ameliorate cortical microcircuit burst firing. The molecular determinants of the dysregulation of activity-dependent BDNF expression by mutant htt appear to be distinct from previously elucidated mechanisms, as they do not involve known NRSF/REST-regulated promoter sequences, but instead result from dysregulation of BDNF exon IV and VI transcription. These data elucidate a novel HD-related deficit in BDNF gene regulation as a plausible mechanism of cortical neuron hypoconnectivity and cortical function deficits in HD. Moreover, the novel model paradigm established here is well-suited to further mechanistic and drug screening research applications.

Introduction

HD is an autosomal dominantly inherited neurodegenerative disorder resulting from a CAG repeat expansion mutation leading to the abnormal elongation of a polyglutamine tract in htt, a multifunctional cellular protein (Bates, 2002). Specific clinical manifestations of HD involve motor and cognitive impairments, including chorea, depression, and/or difficulties in decision-making. At the cellular level, HD appears to arise from neurotoxicity involving a state of cellular dysfunction preceding cell death. During this process, intracellular exposure to mutant htt and N-terminal htt fragments containing the expanded polyglutamine domain lead to protein aggregation, abnormalities in cellular signaling and trafficking, and the dysregulation of gene expression (Luthi-Carter, 2007).

While it is established that HD brain neuropathology involves the striatum and cerebral cortex, the specific impact that mutant htt has on local versus network-level neurophysiology remains less clear. A great deal of emphasis has been placed on understanding changes in the behavior of corticostriatal synapses, focusing particularly on dysfunction and death of striatal cells (Cepeda et al., 2007). In contrast, specific electrophysiological abnormalities of cortical microcircuits arising from the presence of expanded polyglutamine proteins are much less well understood. The mechanisms underlying cortical dysfunction are of high interest because the cognitive and personality changes in HD could readily be explained by abnormal intracortical circuits. Motivated by this hypothesis, we set out to determine the relationship of molecular and synaptic

changes in cortical microcircuits exposed to mutant htt fragments as a basis for inferring HD-related events.

While many animal and cell line-based models of HD exist, there is a need for additional cellular models of HD in which mutant htt's effects on neuron-specific functions can be studied. Such models would be important for achieving a better mechanistic understanding of disease etiology and also to improve the prioritization of lead compounds and candidate drug targets identified in high-throughput screens (Heitz et al., 2008). Having noted the absence of a cellular model for simultaneous measurements of molecular and synaptic effects of mutant htt in cortical neurons, we established a new system to be able to address these issues. Here we report results based on the implementation of a novel *in vitro* cortical neuron model of HD and the combined use of this model and extracellular multielectrode array (MEA) recordings. At the molecular level, the model allowed us to elucidate a novel activity-dependent aspect of mutant htt-related gene dysregulation. MEA recording data also demonstrated the model's utility in elucidating early disease-related changes in neuronal network behavior. We further show how this system might be used to identify pharmacologic agents that overcome specific deficits in neuronal connectivity.

JPET Fast Forward. Published on July 12, 2010 as DOI: 10.1124/jpet.110.167551
This article has not been copyedited and formatted. The final version may differ from this version.

Methods

Cell cultures

Cortical cells from E16-E19 Wistar rat embryos (Charles River, France) were prepared and cultured as described previously (Van Pelt et al., 2004). Cells were plated on multielectrode arrays (MEAs) and/or culture dishes, with prior surface coating by polyethylenimine (10mg/ml, Fluka) and laminin (0.02mg/ml, Gibco) in Neurobasal medium (MEAs) or poly-L-lysine (0.01%) in water (culture dishes), respectively. Plating density was 1'500 cells/mm^2 for MEAs, allowing for quick network formation and high multichannel electrophysiological recordings efficiency (Gambazzi, Markram, and Giugliano, unpublished observations). A lower density of 500 cells/mm^2 was used for culture dishes, to facilitate cell counting and morphological analysis. Medium containing Neurobasal, 2% B-27 supplement (GIBCO, Invitrogen Corporation, ref. 17504) and 10% horse serum (from GIBCO, Invitrogen Corporation, ref. 16050-130) was changed three times per week by removing 0.7 ml and adding 1 ml of fresh medium. Where indicated recombinant human BDNF (R&D Systems, Minneapolis, MN, USA) at a concentration of 50ng/ml was added to the medium twice a week starting from *in vitro* day 4. While concentrations of exogenous BDNF treatment have varied between 2-100 ng/ml in the literature, a concentration of 50ng/ml has been shown to be neuroprotective in a striatal lentiviral model of HD (Zala et al., 2005). Moreover, this concentration assures that the twice weekly addition to the medium is sufficient to achieve a chronically increased level of BDNF. Recordings were performed at least 24 h after medium changes except as indicated (for experiments with the trkB inhibitor K252a).

Lentiviral vector production and infection

Plasmids encoding the first 171 amino acids of mutated htt (htt171-82Q) or wild-type htt (htt171-18Q) under the control of a tetracycline-regulated element promoter, or the tetracycline-regulatable transactivator (tTA1) under the control of a phosphoglycerate kinase promoter were used to prepare self-inactivating lentiviral vectors (Figure 1A) as described previously (Regulier et al., 2003). Lentiviral particles were re-suspended in phosphate-buffered saline (PBS) + 1% bovine serum albumin and the particle content of viral batches was assessed by p24 ELISA (RETROtek, Gentaur, Paris, France). On the day following cell plating, cultures were infected with lentiviruses at ratios of 150 ng p24/1000 cells (tTA1) and 120 ng p24/1000 cells (htt171-82Q or htt171-18Q) (Figure 1B). While the use of full-length htt models may reproduce additional features of HD etiology, the use of N-terminal htt fragments has comprised an important and widely used strategy to approximate the effects of mutant htt.

Multielectrode arrays (MEAs)

Commercial MEAs with planar TiN substrate electrodes (MultichannelSystems, Reutlingen, Germany) were employed for *ex vivo* chronic multisite extracellular recordings. Substrate electrodes had a diameter of 30 µm (Figure 1F), and were organized in an 8x8 square grid with 200 µm spacing. Cell maintenance and electrophysiological recordings were performed at 37°C, 9% O_2, 5% CO_2, and 65% R.H. (Potter and DeMarse, 2001), inside a low-humidity incubator comprising an electronic-friendly environment (Jouan IG750, ThermoFischer Scientific, Waltham, MA, USA). MEA electrodes had an impedance of 100kΩ (in PBS). Electronic amplifiers (MultichannelSystems, Reutlingen, Germany) had a standard gain of 61.6dB, between

10Hz and 3kHz (filters + - 60dB/dec), and large input-impedance ($10^{11}\Omega$ in parallel to 10pF).

MEA data acquisition and analysis

After 5 min of accommodation time following the mounting of each MEA inside the recording setup, spontaneous electrical activity from the cultured neurons was detected, amplified, and recorded at each of the 60 substrate extracellular electrodes simultaneously for 30 min at 20kHz/channel. Recorded traces consisted in multiunit activity, directly related to the firing of action potentials by the neurons in the proximity of each electrode. MCRack software (MultichannelSystems, Reutlingen, Germany) was used to acquire and store the data (9Gb/session, split into ~2Gb files), which were processed off-line channel by channel. Raw voltage waveforms (Figure 1F) were digitally filtered between 150Hz and 2.5kHz and fully rectified. The occurrence of an action potential at a given electrode was identified by a peak-detection algorithm, based on the crossing of an adaptive threshold, as in the LimAda algorithm. Recorded events included the time-stamp of the spike, the index of the electrode where it was detected, and the preceding 200ms and following 800ms of the corresponding raw voltage trace. The occurrence and duration of epochs of synchronized firing (i.e. bursts of spikes; see Figures 1F-G) were identified and detected as in (van Pelt et al., 2004), by post-processing the spike-time histograms (STH). This made it possible to distinguish between epochs of asynchronous spiking activity and epochs of population-wide bursting. During each recording session, the overall number of bursts, the statistics of the inter-burst time intervals, and the number of individual spike that composed each burst were employed as observables of the network-level emerging spontaneous activity

of the cultured neurons (Figure 2, Figure 5A-D). Data are expressed as the mean ± S.E.M. Student's *t*-test and the Kolmogorov-Smirnov test were used to assess the significance ($p<0.05$) of differences in averages and cumulatives, respectively. Pair-wise correlations between intra-burst spike-trains were evaluated as the peak amplitude of the spike-triggered cross-correlograms over a fixed time window (varied in the range 1ms – 1s).

The conclusions reported here are based on repeated observations collected by MEAs on 14 htt171-82Q- and 23 htt171-18Q-expressing (sister) cultures.

Immunostaining and image analysis

Cultures were washed with PBS and fixed in 4% paraformaldehyde (Fluka/Sigma, Buchs, Switzerland) or in methanol (Merck, Germany) for PSD95 staining for 10 min at 4°C. Cultures were incubated with NeuN (1:500, Chemicon, Temecula, CA) or 2B4 (1:500 Millipore, Zug, Switzerland), PSD95 (1:200, Affinity Bioreagents, Golden, CO) and neuronal class III beta-tubulin Tuj1 (1:2000, Covance, Emerville, CA) antibodies in PBS containing 10% normal goat serum (NGS, Gibco, Invitrogen, Basel, Switzerland) and 0.1% Triton X-100 (TX, Fluka, Sigma, Buchs, Switzerland). Cultures were rinsed three times in PBS and then incubated for 1 hour with fluorescent goat anti-mouse secondary antibodies (for NeuN: 1:1000 Cy3-conjugated antibody from Jackson Immunoresearch Laboratories, WestGrove, PA; for 2B4: 1:1000 Alexa Fluor® 488-conjugated antibodies from Invitrogen, Basel, Switzerland, for Tuj1: 1:1000 Alexa Fluor® 594-conjugated antibody from Invitorgen, Basel, Switzerland). Where indicated cultures were stained with Hoechst 33342 dye (Invitrogen, Basel, Switzerland). Images of NeuN-labeled cultures (n=5 or 6 per condition) were acquired using BD Pathway 855 (BD

JPET Fast Forward. Published on July 12, 2010 as DOI: 10.1124/jpet.110.167551
This article has not been copyedited and formatted. The final version may differ from this version.

Biosciences, San Diego, USA) microscope under non-saturating exposure conditions, using the same acquisition settings for all samples in a given experiment. Images of PSD95, 2B4 and Tuj3 stained cultures were acquired using laser-scanning confocal microscope (TCS-SP2 AOBS, Leica Microsystems, Wetzlar, Germany), using the same acquisition settings for all samples in a given experiment unless specifically noted otherwise. Counting of NeuN-positive nuclei and PSD95-positive punctae was performed with ImageJ software (NIH, Bethesda, MD, USA) applying intensity and size thresholds.

TrkB inhibitor experiments

Experiments were initiated on cultures prepared on MEAs (n=9) starting at 14 DIV. Spontaneous activity was recorded for 30 min in three sessions. The first comprised recordings of all cultures 5 hours prior to initiating pharmacologic treatments. The second comprised recordings of all cultures 45 minutes after treatments with TrkB inhibitor K252a (Sigma cat. K1639) at a concentration of 10nM to 3 cultures, at 100nM to 3 separate cultures, and maintaining 3 untreated cultures as controls. A third session recorded the behavior of all three groups of cells one day later (at 15 DIV). Analyses of MEA recordings were performed as indicated above.

Mathematical model of a cultured neuron network

A simplified spike-rate model accounting for the patterned electrical activity emerging in populations of cultured neurons was defined and computer-simulated to interpret the electrophysiological recordings. We described the firing rate *R(t)* of the ensemble of cortical neurons in terms of the single-cell *f-I* curve and of recurrent connectivity

(Giugliano et al., 2008; La Camera et al., 2008). The model replicates some of the features characterizing the population bursts as transient irregular outbursts in *R(t)*. Full details and the source code are provided as a ModelDB entry (https://senselab.med.yale.edu/ modeldb/ShowModel.asp?model=125748).

BDNF RNA measurements

Neuronal stimulation was performed 1.5 weeks after infection with LV. In order to reduce endogenous synaptic activity and prevent calcium entry through NMDA receptors, cortical neurons were pretreated for 30 min with 1 µM tetrodotoxin (Alexis), 100 µM d-(−)-2-amino-5-phosphonopentanoic acid, D(-)-AP-5 (Sigma), and 40 µM 6-cyano-7-nitroquinoxaline-2,3-dione, CNQX (Sigma). To increase the specificity of the stimulations, neurons not subjected to stimulation were exposed to 10 µM nifedipine (Sigma) and 20 µM N-[2-(p-Bromocinnamylamino)ethyl]-5-isoquinolinesulfonamide·2HCl, H-89 (Calbiochem). Where indicated, neurons were stimulated for 90 min with 10 µM forskolin (Calbiochem) and 30 mM KCl. Total RNA was extracted using the RNeasy kit (Qiagen) and 800 ng of total RNA were used for cDNA synthesis employing High Capacity cDNA RT kit (Applied Biosystems). Quantitative real-time PCR was performed on a 7900HT Real-Time PCR System with SDS 2.3 software (Applied Biosystems) using Power SYBR green PCR master mix (Applied Biosystems). Relative expression (V) was calculated by normalization of BDNF to ß-actin expression as described in (Zucker et al., 2005). All qPCR reactions were performed in triplicate. Primers used in this study were based on previous assays (Chen et al., 2003; Kobayashi et al., 2008) and are listed in Table 1.

Results

In order to create a physiologically and molecularly tractable system for assessment, we employed lentiviral gene transfer to develop a novel *in vitro* model of HD-related cortical dysfunction. This involved using HIV-1-derived vectors to express the first 171 amino acids of wild-type or mutated human htt under the control of a tetracycline response element-containing promoter (Rudinskiy et al., 2009; Figures 1A,B) to achieve high transduction efficiency and high levels of transgene expression in rat primary cortical neurons. The expression levels of huntingtin obtained with this approach are much higher than in transgenic mice but still lower than in acutely transfected cells or inducible cell lines. Immunodetection with an anti-polyglutamine antibody (2B4, see Methods) showed that cultures expressing htt171-82Q accumulated the transprotein in the nuclear compartment (Figure 1C) and developed neuritic htt inclusions (Figure 1D) within 10-14 days after lentiviral transduction, whereas cultures expressing htt171-18Q exhibited only weak and diffuse, primarily non-nuclear, labeling (Figure 1C). As assessed by the numbers of NeuN-positive nuclei, the neuronal viability in htt171-82Q-expressing cortical cultures showed no diminution compared to htt171-18Q-infected controls up to 3 weeks *in vitro*, but showed a progressive loss of neuronal cells at later timepoints (≥3.5 weeks) (Figure 1E).

By replacing conventional cell culture dishes with glass-based arrays of 60 substrate microelectrodes (MEAs) (Marom and Shahaf, 2002; Van Pelt et al., 2004), we monitored the effect of mutant htt fragment expression on cortical neuron network activity. Whereas htt171-82Q- and htt171-18Q-expressing cells were indistinguishable at early

timepoints (≤2 weeks), we began to see disturbances in collective neuronal spiking activity in htt171-82Q-expressing cells between 2 and 3 weeks *in vitro* (Figure 2). The fact that the collective firing behavior in htt171-82Q- and htt171-18Q-expressing cultures was similar initially suggests that the htt171-82Q protein does not have a major effect on *ex vivo* neuronal development. Direct inspection of raw MEA voltage recordings revealed a prominent temporal organization of spontaneous electrical activity in the form of bursts of spikes in htt171-82Q- and htt171-18Q-expressing cells (and also in uninfected cells; see below). These properties are similar to those described for *ex vivo* neocortical preparations by other investigators (for review see (Marom and Shahaf, 2002)). After each recording session, single-unit activity was detected at each electrode by an adaptive threshold algorithm (see Methods). The occurrence of individual spike times for each MEA electrode was then represented as a raster plot and summarized as spike-time histograms (STHs) (Figures 1F,G and 2A). These histograms estimate the instantaneous firing rate across all recording sites binned in constant time intervals (≤1 sec). PBs were then identified as increased synchronous firing epochs and detected as peaks in the STH (Van Pelt et al., 2004) (Figure 2A). The PB duration was conventionally defined and estimated as the interval during which the instantaneous firing rate persisted above 5% of its local peak amplitude, computed by means of the raster plot for better temporal accuracy.

As expected, our system was able to detect mutant htt fragment effects on cortical neurons. The mean spike and PB numbers and the distribution of the inter-burst-intervals (IBIs) differed significantly between htt171-18Q and htt171-82Q cultures (Figure 2A-B), with spikes and PBs being significantly less frequent in htt171-82Q

neuronal networks (Figure 2B,D). In contrast, the average fraction of asynchronous (i.e. inter-burst) firing showed no difference between the two conditions (Figure 2B). These observations suggest a specific impairment (or impairments) of network communication underlying PB ignition, and not a change in cell excitability in the HD model. This stereotypical character of PBs was further confirmed in both the disease and control conditions by comparing the cumulative distributions of PB duration and of the inter-burst-interval (Figure 2C,D). In addition, the overall number of action potentials participating in each PB (*i.e.* the intra-burst firing) revealed no significant difference between htt171-82Q- and htt171-18Q-expressing cells (Figure 2E).

Taking into account the fact that htt171-82Q expression was neither accompanied by cell loss nor by decreased intra-burst firing, we interpreted the observed electrophysiological dysfunctions as being neither the result of decreased spiking excitability nor of reduced electrode spike transduction. These interpretations were further supported by the facts that both synchronous/bursting and asynchronous modes of firing demonstrated similar features in the mutant and wild-type cultures (Figure 2). The simplest interpretation of these observations was provided by computer-simulating a mathematical model of an *ex vivo* cortical network (see Methods). In this model, irregular PBs emerge as spontaneous transitions between a “resting” (i.e. asynchronous firing) state and an “excited”, transiently self-sustaining (i.e. synchronous firing) state (Giugliano et al., 2008). Although impairments in intrinsic excitability, such as the spike-frequency adaptation mediated by calcium-dependent outward currents, would interfere with PB by affecting its duration, the model predicts that the frequency (not the duration)

of spontaneous PB occurrence depends on the recurrent excitatory connectivity and on the efficacy of the synaptic coupling between neurons.

We also evaluated pair-wise correlations among spike trains as an indirect measure of the degree of functional connectivity in the network (Perkel et al., 1967). Assessed across all possible MEA electrode pairs, we found weak correlations between the firing activity in both in htt171-82Q and htt171-18Q cultures. However, pair-wise correlations were significantly smaller in the HD model then control (Figure 2F), while no qualitative difference was observed when the (decreasing) relationship between correlation and inter-electrode pair distance was evaluated (Figure 2G).

Overall, the above modeling and recording results suggested that a discrete subset of electrophysiologic measures differentiate htt171-82Q- and htt171-18Q-expressing cells. Specifically, the rate of PB occurrence and the spike-train correlations are significantly decreased in htt171-82Q- compared to htt171-18Q-expressing cells, consistent with a deficit in synaptic connectivity rather than a decrease in intrinsic excitability. This is also accompanied by a lower number of total spikes in the htt171-82Q-expressing cultures. In contrast, the spontaneous emergence of PBs (stereotypical of recurrent glutamatergic synaptic interactions in random networks (Marom and Shahaf, 2002)) and PB spreading to the entire network demonstrated similar characteristics in htt171-82Q and htt171-18Q cells. Likewise, the synaptic and/or cellular dynamics underlying PB termination (generally termed activity-dependent fatigue by intracellular ion accumulation or neurotransmitter ready-releasable pool exhaustion), was also similar in htt171-82Q and

htt171-18Q cultures (as evidenced by the number of spikes / PB and the PB duration remaining unaffected).

We next considered the molecular mechanism of the electrophysiologic phenotype in the mutant htt-exposed cortical cells. One possible explanation for the observed decrease in PB firing behavior would be an underlying defect in synaptic reinforcement. Since BDNF is an important regulator of synaptic plasticity, and loss of BDNF function has been previously implicated in HD, we assessed whether a deficiency of BDNF expression could explain the observed cortical microcircuit phenotype.

We first determined whether BDNF signaling through TrkB receptors was an important determinant of PB firing in our cortical neuron-based system. We addressed this question by assessing whether short-term application of the TrkB inhibitor K252a would suppress PB activity in the MEA cultures. In agreement with our expectations, short-term K252a treatment resulted in a dose- and time-dependent loss of PB firing (Figure 3), without influencing neuronal viability (as determined by NeuN counts, data not shown). These results support the hypothesis that decreased BDNF activity might underlie the observed diminution of function observed in htt171-82Q cells.

To address this hypothesis, we first determined whether BDNF expression was altered in htt171-82Q-exposed neurons in a timeframe consistent with its driving the observed electrophysiologic abnormalities. Therefore, BDNF expression was measured in both resting and depolarizing conditions at timepoints preceding or coincident with altered network behavior. Interestingly, the earliest detected change was a deficit in activity-

dependent induction of BDNF expression, which occurred at 10 days *in vitro* (Figure 4A), *i.e.* prior to timepoints at which htt171-82Q- and htt171-18Q-expressing cells could be differentiated on the basis of PB firing. These results suggested that a deficit in activity-dependent BDNF gene regulation might be responsible for diminished cortical microcircuit activity in HD cells.

In order to determine whether BDNF levels could influence the network behavior in the predicted direction, we tested whether increasing BDNF availability could reverse the abnormal PB firing behavior observed in HD cells. Consistent with our hypothesis, adding exogenous BDNF to the culture medium normalized the PB frequencies and IBI intervals of htt171-82Q-exposed cells, leading to significantly increased PB frequencies and decreased IBIs compared to non-BDNF-treated sister cultures (Figure 5). Indeed, the restoring effect on PB timing by BDNF was readily apparent (Figure 5A) and extended to both the IBI (Figure 5C) and duration distributions (Figures 5B). Quantified in terms of numbers of individual action potentials, BDNF did not completely restore the size of individual PBs, however (Figure 5D). Comparing samples of individual PBs recorded in treated and untreated htt171-82Q-exposed sister cells, their distribution is significantly shifted towards equally long PBs but slightly less populated by individual action potentials (see Figure 2E and Figure 5D). Taken together, these results support that decreased activity-dependent BDNF expression is a mediator of the cortical microcircuit hypoconnectivity in HD-affected cells.

To further address the effect of impaired activity-dependent BDNF expression on synaptic connectivity in our model, we considered possible changes in the relative

JPET Fast Forward. Published on July 12, 2010 as DOI: 10.1124/jpet.110.167551
This article has not been copyedited and formatted. The final version may differ from this version.

numbers of synapses in htt171-82Q cells (Figures 5E,F). These were assessed by quantifying numbers of PSD95-positive structures as an indicator of postsynaptic specializations. Indeed, Htt171-82Q-expressing cells demonstrate a significant decrease in PSD95-positive bouton-like punctae, which is reversed by BDNF treatment. These results suggest that the structural organization of synapses is one parameter of cortical microcircuit connectivity that may be affected by BDNF availability in HD cells.

We subsequently considered the mechanism by which mutant htt fragments dysregulated activity-dependent BDNF expression. Previous studies have shown that increased NRSF/REST activity at the BDNF exon II promoter could mediate an HD-related decrease in BDNF expression (reviewed in Zuccato and Cattaneo, 2007). Further, it has been shown that NRSF/REST can also regulate the transcription of BDNF exon I and regulation has been also inferred for the transcription of BDNF transcript III (reviewed in Zuccato and Cattaneo, 2007). We therefore undertook exon-specific BDNF RNA analyses to determine the whether an NRSF/REST-related mechanism could account for the decreased activity-dependent BDNF expression observed in our HD model system. We present these results adopting the rat BDNF gene nomenclature proposed by (Aid et al., 2007). Although BDNF I, IIC, and III mRNAs showed an activity-dependent induction, the levels of these RNAs were not significantly different between htt171-82Q- and htt171-18Q-expressing cells (Figure 4C). These results suggest that another mechanism accounts for polyglutamine-related differences in activity-dependent BDNF expression. Upon examining additional BDNF transcripts, we discovered that differences in activity-dependent BDNF gene regulation could be attributed specifically to the differential expression of BDNF IV and VI mRNAs (Figure

4B). (It should be noted that transcript VI has also been referred to as transcript V in the rat, mouse and human BDNF gene structure (see Pruunsild et al., 2007) as is the case in previous HD studies (Benn et al., 2008; Zuccato et al., 2008)). These results indicate the existence of NRSF/REST-independent effect(s) of mutant htt fragments may cause an early deficit in activity-dependent expression of BDNF RNA by cortical neurons. Moreover, this novel aspect of BDNF gene dysregulation meets the temporal and pharmacologic criteria to support its involvement in abnormal cortical microcircuit behavior.

Discussion

While the striatum has been more noted for its early degeneration in HD, the cerebral cortex also shows significant atrophy and has been implicated in striatal neuron death through evidence of increased glutamatergic tone, leading to excitotoxicity, and decreased neurotrophic support (Zuccato and Cattaneo, 2007). Likewise, corticocortical connections are also important for cortical network behavior and cortical output, and specific neuronal populations as well as the corpus callosum show significant atrophy in HD (Thu et al., 2010; Rosas et al., 2008; Rosas et al., 2010). Therefore, studies of cortical neuron dysfunction have great potential relevance for both cortical and striatal effects of HD. In addition, synaptic effects of mutant htt are more easily studied in an excitatory neuron system where activity spontaneously arises without chemical or electrical intervention. The present model therefore comprises a rational and unique system for further analysis and dissection of HD-related effects on synaptic function and screening of synapse-targeted therapeutics.

The spontaneous activity emergence and transition from uncorrelated to clustered (i.e. PB) firing activity studied here is a very common feature of *ex vivo* neuronal networks (Van den Pol et al., 1996). In the present work, we considered mutant huntingtin's effects at timepoints within the first 2-3 weeks *in vitro* because we aimed to study early network-level dysfunction in the absence of the confounding effects of cell loss. Since the spontaneous firing behavior of htt171-18Q and htt171-82Q cultures arises similarly at early timepoints and diverges subsequently, we believe that the polyQ-related

differences in electrophysiological phenotype are not due to effects on neuronal differentiation *ex vivo*.

The implication of abnormal glutamate neurotransmission in HD is a long-standing issue (Fan and Raymond, 2007). Thus, in some respects, it is surprising that mutant htt-exposed cortical neurons would show decreased rather than increased excitatory synaptic activity. This is in contrast to a simple excitotoxicity theory of HD-related neurodegeneration based on dysregulated cortical glutamate release or increased striatal responses to physiologically normal levels of transmitter. However, neither our results nor previous reports of lack of enhancement of excitotoxic phenomena in HD systems (Fan and Raymond, 2007) rule out that a more complex dysfunction of glutamatergic output from cortical neurons might result in excitotoxic sequellae in the cortex or striatum *in vivo*.

A tight relationship between glutamatergic neurotransmission and network-level spontaneous activity has been defined in cortical cultures previously (for a review see Marom and Shahaf, 2002). At the single-cell level, BDNF has been shown to acutely potentiate glutamatergic transmission by acting postsynaptically, for example via regulation of glutamatergic receptor subunit trafficking (Yoshii and Constantine-Paton, 2007; Nakata and Nakamura, 2007). Our data are consistent these previous observations by showing that BDNF is an important determinant of burst firing behavior and regulates PSD-95-positive synaptic bouton number in primary cortical neurons.

Although BDNF normalized one major aspect of cortical microcircuit dysfunction in our HD model system (PB firing), it did not completely reverse polyQ htt effects. Specifically, the number of total spikes remained lower in htt171-82Q cells despite BDNF treatment. The lower spike number in htt171-82Q cells also persisted despite a BDNF-mediated increase PSD95-positive boutons. The reduced spike occurrence frequency could be attributed to abnormalities in voltage-gated sodium channels (Oyama et al., 2006), intracellular calcium dynamics (Bezprozvanny et al., 2007), potassium channels (Hodges et al., 2006), and even toxic voltage-independent increased membrane permeability (Kagan et al., 2001) all of which comprise previously identified HD-related phenomena. Nevertheless, the stereotypical features of PBs (Figure 2B,C,E), and the altered spike-timing cross-correlations (Figure 2F-G) are best explained by synapse-related dysfunction(s).

Our observed behaviors of htt171-82Q-expressing neurons are also in line with previous observations of HD brain. On the molecular level, we and others have shown changes in the expression of synaptic proteins (Morton and Edwardson, 2001; Luthi-Carter et al., 2003; Hodges et al., 2006; Smith et al., 2007). Electrophysiologic data have also shown impairments in cortical function in HD mice (reviewed in Cepeda et al., 2007). Extracellular recordings in awake behaving animals also found significant reductions in the rate and synchrony of spontaneous burst firing in the cortices of HD compared to wild-type mice (Walker et al., 2008); moreover, the same study reported no change in burst duration; all of these findings are consistent with our observations. On the other hand, recordings in cortical slices from R6/2 mice by patch-clamp electrophysiology

(Cummings et al., 2009) show a more complex profile of connectivity deficits. In the latter study, both excitatory and inhibitory synaptic projections onto cortical pyramidal neurons were defined during two stages of the disease: an asymptomatic stage (P21), and a stage considerably after emergence of overt behavioral symptoms (P80). At P80, the authors report seizure-prone cortical microcircuitry (characterized by increased efficacy, release probability, and connectivity probability in glutamatergic synapses and weaker in efficacy, release probability, and connectivity probability in GABAergic synapses), rather the opposite of what we detected *in vitro*. However, in recordings before P21, the same group showed that the synaptic abnormalities are approximately reversed (downregulated excitation and upregulated inhibition). At first approximation, this early stage parallels our results and predictions *in vitro*, and therefore, it is possible that our HD cortical model may best represent early-stage disease-related dysfunction. Another possible connection is provided by changes in BDNF expression (see below), which might explain the phenotype of later-stage mice as decreased BDNF-mediated facilitation of GABAergic neurotransmission (Hong et al., 2008; Sakata et al., 2009). Taken together, the present data suggest a complex dysregulation of neuronal firing behavior and circuitry in the HD cortex, with both BDNF-driven and other components.

The present study provides new evidence that decreased BDNF expression, particularly activity-dependent BDNF expression, is an early and relevant event underlying PB dysfunction. HD-related decreases in BDNF expression and trafficking have been explored in previous work (for a review see Zuccato and Cattaneo, 2007). The effect of another polyglutamine disease protein, mutant atrophin-1, on depolarization-dependent *BDNF* promoter activity has also been explored in an *in vitro* system (Miyashita et al.,

2005). The present data are consistent with previous reports, yet several aspects of the present work extend the current understanding in novel and potentially important ways. The first is to elucidate and emphasize the important effects that BDNF deprivation may have on cortical microcircuits (rather than striatal neuron survival) in HD. The second is to show that the activity-dependent component of BDNF expression is affected by mutant htt. The third is to provide evidence that the earliest deficit in *BDNF* gene dysregulation occurs via a non-REST/NRSF-mediated mechanism (a finding that is paralleled by previous exon-specific BDNF transcript analyses, which show deficiencies in the orthologous BDNF transcripts in R6/2 mouse and human HD brains (which are, due to differences in nomenclature conventions, referred to as transcripts IV and V in these studies (Benn et al., 2008; Zuccato et al., 2008).

While mechanisms of activity-dependent transcription from the exon VI promoter have not been extensively studied, several mechanisms have been implicated in the activity-dependent transcription of exon IV (for a recent review see Greer and Greenberg, 2008). These include the phosphorylation and DNA binding of the CRE-binding protein (CREB), the recruitment of CREB-associated cofactors including CBP and TORC1, the phosphorylation-mediated release of transcriptional repression imparted by the methylated DNA binding protein MeCP2, direct promoter DNA demethylation, and positive regulatory activity of MEF2C. Given the important role attributed to the activity-dependent component of BDNF expression, these known mechanisms of exon IV regulation pose hypotheses meriting evaluation in HD.

Beyond understanding specific mechanisms of htt toxicity, there is also a pressing need for HD models that can be employed to rapidly and accurately screen candidate drugs capable of rescuing neuronal function. The majority of currently used *in vitro* HD models are designed to examine cell survival or protein accumulation abnormalities, which may represent late stages of disease or be of uncertain relevance to addressing clinically meaningful endpoints. Moreover, the implementation of cortical cells for this assay not only facilitates the study of patterned network activity (which arises spontaneously in excitatory neurons), but also provides a system complementary to striatal cells in which to examine and potentially remediate mutant htt's effects. While animal models of HD may be more faithful to the complex cellular and network relationships underlying human disease, their throughput rate for drug screening is low. Here we present the possible alternative implementation of an *in vitro* HD model coupled to MEAs as a simple way to probe neuronal network function upstream of neuronal cell death. Electrophysiological MEA recordings seem ideally implemented for secondary screening purposes, comprising a rapid and repeatable longitudinal assay. Here we show proof-of-concept evidence that our system can successfully detect a disease-modifying effect (whose therapeutic benefit has been shown previously in transgenic HD mice (Cepeda et al., 2004; Lynch et al., 2007; Gharami et al., 2008; Giralt et al., 2009)). In a broader context, one can also envisage the utility of MEA-integrated disease models to study and develop therapies for a wide range of neurological conditions.

JPET Fast Forward. Published on July 12, 2010 as DOI: 10.1124/jpet.110.167551
This article has not been copyedited and formatted. The final version may differ from this version.

Acknowledgements

We express our sincere thanks to Drs. M. Pignatelli, G. La Camera and J.-R. Cardinaux for helpful discussions, to Drs. J. Van Pelt, B.R. Miller, W.L.C. Rutten, A. Tscherter, J. Streit, M Chiappalone, V. Pasquale, and S. Martinoia for critical comments on an earlier version of the manuscript, and to M. de Fatima Rey, S. Garcia, and K. Antoniello for excellent technical support.

References

Aid T, Kazantseva A, Piirsoo M, Palm K, and Timmusk T (2007) Mouse and rat BDNF gene structure and expression revisited. *J Neurosci Res.* **85**: 525-35.

Bates GP, Harper P, and Jones L (2002) *Huntington's Disease*. 3rd ed. Oxford University Press, Oxford.

Benn CL, Fox H, and Bates GP (2008) Optimisation of region-specific reference gene selection and relative gene expression analysis methods for pre-clinical trials of Huntington's disease. *Mol Neurodegener* **3:** 17.

Bezprozvanny I (2007) Inositol 1,4,5-tripshosphate receptor, calcium signalling and Huntington's disease. *Subcell Biochem* **45:** 323-335.

Cepeda C, Starling AJ, Wu N, Nguyen OK, Uzgil B, Soda T, André VM, Ariano MA, and Levine MS (2004) Increased GABAergic function in mouse models of Huntington's disease: reversal by BDNF, *J Neurosci Res* **78**: 855-67.

Cepeda C, Wu NP, Andre VM, Cummings DM, and Levine MS (2007) The corticostriatal pathway in Huntington's disease. *Prog Neurobiol* **81:** 253-271.

Chen WG, Chang Q, Lin Y, Meissner A, West AE, Griffith EC, Jaenisch R, and Greenberg ME (2003) Derepression of BDNF transcription involves calcium-dependent phosphorylation of MeCP2. *Science* **302:** 885-889.

Cummings DM, Andre VM, Uzgil BO, Gee SM, Fisher YE, Cepeda C, and Levine MS (2009) Alterations in cortical excitation and inhibition in genetic mouse models of Huntington's disease. *Journal of Neuroscience* **29:** 10371-10386.

Fan MMY and Raymond LA (2007) N-methyl-D-aspartate (NMDA) receptor function and excitotoxicity in Huntington's disease. *Prog Neurobiol* **81:** 272-293.

Gharami K, Xie Y, An JJ, Tonegawa S, and Xu B (2008) Brain-derived neurotrophic factor over-expression in the forebrain ameliorates Huntington's disease phenotypes in mice. *J Neurochem* **105:** 369-379.

Giralt A, Rodrigo T, Martín ED, Gonzalez JR, Milà M, Ceña V, Dierssen M, Canals JM, and Alberch J (2009) Brain-derived neurotrophic factor modulates the severity of cognitive alterations induced by mutant huntingtin: involvement of phospholipaseCgamma activity and glutamate receptor expression. *Neuroscience* **158:** 1234-1250.

Giugliano M, La Camera G, Fusi S, and Senn W (2008) The response of cortical neurons to in vivo-like input current: theory and experiment: II Time-varying and spatially distributed inputs. *Biol Cybern* **99:** 303-318.

Greer PL and Greenberg ME (2008) From synapse to nucleus: calcium-dependent gene transcription in the control of synapse development and function. *Neuron* **59:** 846-860.

Heitz F, La Rosa S, Gonzalez-Couto E, Gaviraghi G, and Terstappen GC (2008) Drug discovery and development for Huntington's disease - an orphan indication with high medical need. *IDrugs* **11:** 653-660.

Hodges A, Strand AD, Aragaki AK, Kuhn A, Sengstag T, Hughes G, Elliston LA, Hartog C, Goldstein DR, Thu D, Hollingsworth ZR, Collin F, Synek B, Holmans PA, Young AB, Wexler NS, Delorenzi M, Kooperberg C, Augood SJ, Faull RLM, Olson JM, Jones L, and Luthi-Carter R (2006) Regional and cellular gene expression changes in human Huntington's disease brain. *Hum Mol Genet* **15:** 965-977.

Hong EJ, McCord AE, and Greenberg ME (2008) A biological function for the neuronal activity-dependent component of Bdnf transcription in the development of cortical

inhibition. *Neuron* **60:** 610-624.

Kagan BL, Hirakura Y, and Azimova R (2001) The channel hypothesis of Huntington's disease. *Brain Res Bull* **56:** 281-284.

Kobayashi H, Yokoyama M, Matsuoka Y, Omori M, Itano Y, Kaku R, Morita K, and Ichikawa H (2008) Expression changes of multiple brain-derived neurotrophic factor transcripts in selective spinal nerve ligation model and complete Freund's adjuvant model. *Brain Res* **1206:** 13-19.

La Camera G, Giugliano M, Senn W, and Fusi S (2008) The response of cortical neurons to in vivo-like input current: theory and experiment : I Noisy inputs with stationary statistics. *Biol Cybern* **99:** 279-301.

Luthi-Carter R (2007) Huntington's and other polyglutamine diseases: many effects of single gene mutations. *Drug Discovery Today: Disease Mechanisms* **4:** 111-119.

Luthi-Carter R, Apostol BL, Dunah AW, DeJohn MM, Farrell LA, Bates GP, Young A B, Standaert DG, Thompson LM, and Cha JHJ (2003) Complex alteration of NMDA receptors in transgenic Huntington's disease mouse brain: analysis of mRNA and protein expression, plasma membrane association, interacting proteins, and phosphorylation. *Neurobiology of Disease* **14:** 624-636.

Lynch G, Kramar EA, Rex CS, Jia Y, Chappas D, Gall CM, and Simmons DA (2007) Brain-derived neurotrophic factor restores synaptic plasticity in a knock-in mouse model of Huntington's disease. *J Neurosci.* **27**: 4424-34.

Marom S and Shahaf G (2002) Development, learning and memory in large random networks of cortical neurons: lessons beyond anatomy. *Quart Rev Biophys* **35:** 63-87.

Miyashita T, Tabuchi A, Fukuchi M, Hara D, Kisukeda T, Shimohata T, Tsuji S, and

Tsuda M (2005) Interference with activity-dependent transcriptional activation of BDNF gene depending upon the expanded polyglutamines in neurons. *Biochemical and Biophysical Research Communications* **333:** 1241-1248.

Morton AJ, and Edwardson JM (2001) Progressive depletion of complexin II in a transgenic mouse model of Huntington's disease. *J Neurochem* **76:** 166-172.

Nakata H, and Nakamura S (2007) Brain-derived neurotrophic factor regulates AMPA receptor trafficking to post-synaptic densities via IP3R and TRPC calcium signaling. *FEBS Lett* **581:** 2047-2054.

Oyama F, Miyazaki H, Sakamoto N, Becquet C, Machida Y, Kaneko K, Uchikawa C, Suzuki T, Kurosawa M, Ikeda T, Tamaoka A, Sakurai T, and Nukina N (2006) Sodium channel beta4 subunit: down-regulation and possible involvement in neuritic degeneration in Huntington's disease transgenic mice. *J Neurochem* **98:** 518-529.

Perkel DH, Gerstein GL, and Moore GP (1967) Neuronal spike trains and stochastic point processes II Simultaneous spike trains. *Biophysical Journal 7*, 419-440.

Potter SM and DeMarse TB (2001) A new approach to neural cell culture for long-term studies. *J Neurosci Methods* **110:** 17-24.

Pruunsild P, Kazantseva A, Aid T, Palm K, and Timmusk T (2007) Dissecting the human BDNF locus: Bidirectional transcription, complex splicing, and multiple promoters. *Genomics* **90**: 397–406.

Régulier E, Trottier Y, Perrin V, Aebischer P, and Déglon N (2003) Early and reversible neuropathology induced by tetracycline-regulated lentiviral overexpression of mutant huntingtin in rat striatum. *Hum Mol Genet* **12:** 2827-2836.

Rosas HD, Lee SY, Bender AC, Zaleta AK, Vangel M, Yu P, Fischl B, Pappu V, Onorato C, Cha JHJ, Salat DH, and Hersch SM (2010) Altered white matter microstructure in

the corpus callosum in Huntington's disease: Implications for cortical "disconnection". *NeuroImage* **49:** 2995-3004.

Rosas HD, Salat DH, Lee SY, Zaleta AK, Pappu V, Fischl B, Greve D, Hevelone N, and Hersch SM (2008) Cerebral cortex and the clinical expression of Huntington's disease: complexity and heterogeneity. *Brain* **131:** 1057-1068.

Rudinskiy N, Kaneko YA, Beesen AA, Gokce O, Régulier E, Déglon N, and Luthi-Carter R (2009) Diminished hippocalcin expression in Huntington's disease brain does not account for increased striatal neuron vulnerability as assessed in primary neurons. *J Neurochem* **111:** 460-472.

Sakata K, Woo NH, Martinowich K, Greene JS, Schloesser RJ, Shen L, and Lu B (2009) Critical role of promoter IV-driven BDNF transcription in GABAergic transmission and synaptic plasticity in the prefrontal cortex. *Proc Natl Acad Sci USA* **106:** 5942-5947.

Smith R, Klein P, Koc-Schmitz Y, Waldvogel HJ, Faull RLM, Brundin P, Plomann M, and Li J-Y (2007) Loss of SNAP-25 and rabphilin 3a in sensory-motor cortex in Huntington's disease. *J Neurochem* **103:** 115-123.

Thu DCV, Oorschot DE, Tippett LJ, Nana AL, Hogg VM, Synek BJ, Luthi-Carter R, Waldvogel HJ, and Faull RLM (2010) Cell loss in the motor and cingulate cortex correlates with symptomatology in Huntington's disease. *Brain* **133:** 1094-1110.

Van Den Pol AN, Obrietan K, and Belousov, A (1996) Glutamate hyperexcitability and seizure-like activity throughout the brain and spinal cord upon relief from chronic glutamate receptor blockade in culture. *Neuroscience* **74:** 653-674.

Van Pelt J, Wolters PS, Corner MA, Rutten WLC, and Ramakers GJA (2004) Long-term characterization of firing dynamics of spontaneous bursts in cultured neural

networks. *IEEE Trans Biomed Eng* **51:** 2051-2062.

Walker AG, Miller BR, Fritsch JN, Barton SJ, and Rebec GV (2008) Altered information processing in the prefrontal cortex of Huntington's disease mouse models. *Journal of Neuroscience* **28:** 8973-8982.

Yoshii A, and Constantine-Paton M (2007) BDNF induces transport of PSD-95 to dendrites through PI3K-AKT signaling after NMDA receptor activation. *Nat Neurosci* **10:** 702-711.

Zuccato C and Cattaneo E (2007) Role of brain-derived neurotrophic factor in Huntington's disease. *Prog Neurobiol* **81:** 294-330.

Zuccato C, Marullo M, Conforti P, MacDonald ME, Tartari M, and Cattaneo E (2008) Systematic assessment of BDNF and its receptor levels in human cortices affected by Huntington's disease. *Brain Pathol* **18:** 225-238.

Zucker B, Luthi-Carter R, Kama JA, Dunah AW, Stern EA, Fox JH, Standaert DG, Young AB, and Augood SJ (2005) Transcriptional dysregulation in striatal projection- and interneurons in a mouse model of Huntington's disease: neuronal selectivity and potential neuroprotective role of HAP1. *Hum Mol Genet* **14:** 179-189.

Footnotes

This work was supported by the European FP6 grant “NEURONANO” [NMP4-CT-2006-031847], the European FP6 ESR training program in “Nervous System Repair”, the Telethon Action Suisse, a CTI award from the Swiss National Science Foundation, the EPFL, the Univ. of Antwerp (NOI BOF), and the Belgian Interuniversity Attraction Pole (IAP P6/29).

LG, OG, TS are equally contributing lead authors

MG, RLC are equally contributing senior authors

Reprint requests:

Ruth Luthi-Carter, EPFL SV BMI LNGF, Station 15, CH-1015 Lausanne

ruth.luthi-carter@epfl.ch

tel: +41 21 693 6533, fax: + 41 21 693 9628

Legends for figures

Figure 1

Lentiviral constructs, *in vitro* model of HD effects on cortical neurons and electrophysiological recordings of spontaneously active ex vivo cortical networks. (A) Lentiviral expression vectors encoding wild-type (18Q) or mutated (82Q) htt fragments under the control of a tetracycline-regulated element promoter containing the Tet-response element (TRE) with seven direct repeats of the tetO operator sequence upstream of a minimal CMV promoter (SIN-TRE-htt171) and encoding the tetracycline-controlled transactivator tTA1 (i.e. tetracycline repressor tetR fused to four copies (4F) of the minimal transcriptional activation domain of VP16) under the control of the PGK promoter. Both vectors (employed as in (Rudinskiy et al., 2009)) were self-inactivating (SIN) and contained a posttranscriptional woodchuck hepatitis B virus regulatory element (WPRE). **(B)** Scheme depicting the experimental timeline. **(C)** Within two weeks in vitro, cortical cultures expressing htt171-82Q show accumulation of huntingtin in the nucleus, as shown by colocalization of huntingtin immunostaining (with antibody 2B4, shown in green in the center and right panels) and nuclear staining (with Hoechst 33342, shown in purple in left panels), as indicated by arrowheads. Identification of the cells as neurons and markage of the non-nuclear compartment of huntingtin-expressing neurons is provided by co-visualization of neuronal tubulin Tuj1 by immunostaining (right panels, indicating merged immunostained 2B4+Tuj1 images). Note that nuclear accumulation of huntingtin is unique to the htt171-82Q condition. The intensity of the 2B4 image of the htt171-18Q-expressing cells has been enhanced to

show the predominantly extranuclear distribution of the labeling, which would be too faint to be observable using the same parameters as for the htt171-82Q image. Scale bar = 25µM. (D) Neuritic inclusion bodies are present in htt171-82Q cells at 2 weeks *in vitro* as shown by the juxtaposition of bright 2B4-positive profiles with Tuj1-positive neurites, as indicated by arrows; scale bar 2µm. **(E)** Counts of NeuN-positive neuronal nuclei in the cultures revealed no significant cell death within three weeks *in vitro*. After four weeks significant cell death is observed in cultures expressing htt171-82Q. Data is presented as percent of control (htt171-18Q) for each time point. Bars represent mean values ± SEM. * $p < 0.05$. **(F)** Cultures on glass arrays of 60 substrate planar microelectrodes (left panel). Each electrode independently detects extracellular action potentials of nearby neurons (right panel). **(G)** Recordings revealed that spontaneous activity consisted of asynchronous firing and rare bursts of events synchronized across MEA electrodes.

Figure 2

Recordings and statistical analyses of spontaneous population bursts (PBs) in control htt171-18Q (n=11) and HD htt171-82Q (n=12) sister cultures. (A) Network-wide spiking activity was detected at 14 days *in vitro* and represented as raster plots as well as spike-time histograms (STHs). These revealed irregular occurrence of epochs of synchronized spiking (i.e. PBs), interleaved with asynchronous firing (see Figure 1G). PBs had similar durations and distributions across the entire MEA surface. In both 18Q and 82Q conditions, only the PB occurrence frequency showed significant differences **(B, D)** (histograms show mean ± SEM, * $p < 0.05$), while inter-burst firing **(B)**, PB duration **(B, C)** and intra-burst firing **(E)** revealed no differences. This suggests that PBs

occur as relatively stereotyped events. Significant differences were also observed in the pair-wise spike-time correlations **(F)** but not in the qualitative dependence on the inter-electrode distances **(G)** (*$p < 0.05$).

Figure 3

Population burst firing is dependent on BDNF signaling. The effect of the TrkB inhibitor K252a on spontaneous activity was assessed at 2 weeks *in vitro*. Three recordings were performed : one 5 hours prior to the K252a addition, one 45 minutes after the addition of K252a (n=3 control MEAs without K252a addition, n=3 MEAs with 10nM K252a and n=3 MEAs with 100nM K252a), and one 24 hours after the addition of K252a (same three conditions). No significant difference in the number of population bursts were observed in the cultures at 14 DIV before adding K252a (left histogram). 45 minutes after adding K252a a significant concentration-dependent reduction of population bursts were observed in K252a treated cultures. After 24 hours the population burst rate of K252a-treated cultures was further reduced compared to control cultures (right histogram). K252a treatments had no effects on neuronal viability under these conditions as measured by NeuN-positive cell counts (data not shown).

Figure 4

Basal and activity-dependent expression of BDNF transcripts. Activity-dependent expression of BDNF transcripts was analyzed in primary cortical cultures (10 DIV) expressing wild-type (18Q) or mutated (82Q) htt fragments. This analysis adopts the rat *BDNF* gene nomenclature proposed by Aid et al., 2007. Activity-dependent effects were assessed by application of 10 µM forskolin (FSK) and 30mM KCl for 90 min. In order to

reduce endogenous synaptic activity and prevent calcium entry through NMDA receptors, cortical neurons were pretreated for 30 min with 1 µM tetrodotoxin, 100 µM d-(−)-2-amino-5-phosphonopentanoic acid and 40 µM 6-cyano-7-nitroquinoxaline-2,3-dione. To increase the specificity of the stimulations, neurons not subjected to stimulation were exposed to 10 µM nifedipine and 20 µM H-89. Relative expression (V-value) was calculated by normalization to ß-actin expression as described in Zucker et al., (2005). All qPCR reactions were performed in triplicate. Bars represent mean values ± SEM, n=5. Black bars represent cultures expressing wt Htt (18Q), empty bars represent cultures expressing mutated Htt (82Q). * $p<0.05$ for the comparison of basal levels of expression; ## $p<0.01$, ### $p<0.001$ for the comparison of induced expression levels. NS - non significant. **(A)** Total BDNF mRNA levels. Activity-dependent increase of BDNF expression is significantly lower in neurons expressing mutated Htt. **(B)** Expression of REST/NRSF-independent exons in response to depolarization is decreased in neurons expressing mutated Htt. **(C)** Activity-dependent component of REST/NRSF-dependent exons is not influenced by mutated Htt.

Figure 5

BDNF treatment improves synaptic connectivity of htt171-82Q cells. (A-D) Shown are recordings and statistical analyses of spontaneous population bursts (PBs) in control htt171-18Q (n=2), and in htt171-82Q sister cultures with (n=6) and without (n=6) BDNF treatment (50ng/ml, added twice weekly). Bars represent the mean value ± SEM; *p < 0.05. **(A)** The irregular occurrence of PBs and their abnormalities in htt171-82Q cells after 23 days *in vitro* were similar to those observed in the experiment described in Figure 2. In contrast, BDNF-treated htt171-82Q cultures showed a significant recovery

compared to the untreated 82Q cells **(A, C, D)**. While the PB duration showed no difference in the three conditions (**A, B**), the PB occurrence frequency was rescued by BDNF treatment in htt171-82Q cells. The decrease in the overall spiking activity in htt171-82Q cells was not rescued by BDNF **(A)**, which showed an even lower mean number of spikes composing PBs. **(E, F)** The number of PSD95-positive punctae is decreased in cultures expressing htt171-82Q (at 3.5 weeks) as compared to cells expressing htt171-18Q (*). In correlation with the improvement of PB firing behavior, BDNF treatment significantly increased the number of PSD95-positive punctae in htt171-82Q cells as compared to untreated htt171-82Q expressing cultures (**). Scale bar 25μM. Bars represent mean values ± SEM, n=15. * $p<0.05$, ** $p<0.01$.

JPET Fast Forward. Published on July 12, 2010 as DOI: 10.1124/jpet.110.167551
This article has not been copyedited and formatted. The final version may differ from this version.

Tables

Table 1

PCR primers used in this study

exon	Forward primer	Reverse primer
I	tgttggggagacgagatttt	cgtggacgtttgcttctttc
IIa	tacttcatccagttccaccag	caagttgccttgtccgt
IIb	aagctccggttccaccag	tgcttctttcatgggcg
IIc	gtggtgtaagccgcaaaga	cgtggacgtttgcttctttc
III	ctgagactgcgctccactc	gtggacgtttgcttctttca
VI	gatccgagagctttgtgtgg	gtggacgtttgcttctttca
IV	cgccatgcaatttccactatcaataatttaac	gtttactttgacaagtagtgactgaaaaag
Universal	tggatgccgcaaaca	ccgggactttctccaggact
b-actin	aggcatcctgaccctgaag	gctcattgtagaaagtgtgg

Figure 1

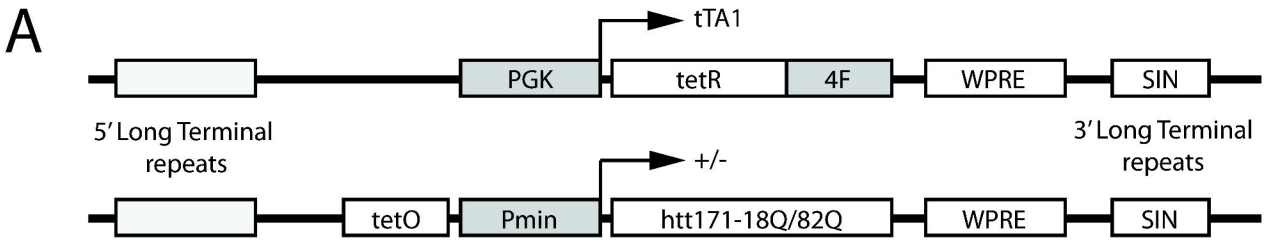
A
tTA1
PGK
tetR
4F
WPRE
SIN
5' Long Terminal repeats
3' Long Terminal repeats
+/-
tetO
Pmin
htt171-18Q/82Q
WPRE
SIN

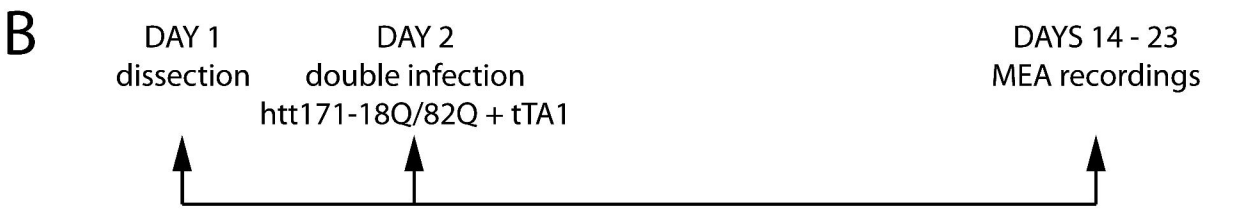
B
DAY 1
dissection
DAY 2
double infection
htt171-18Q/82Q + tTA1
DAYS 14 - 23
MEA recordings

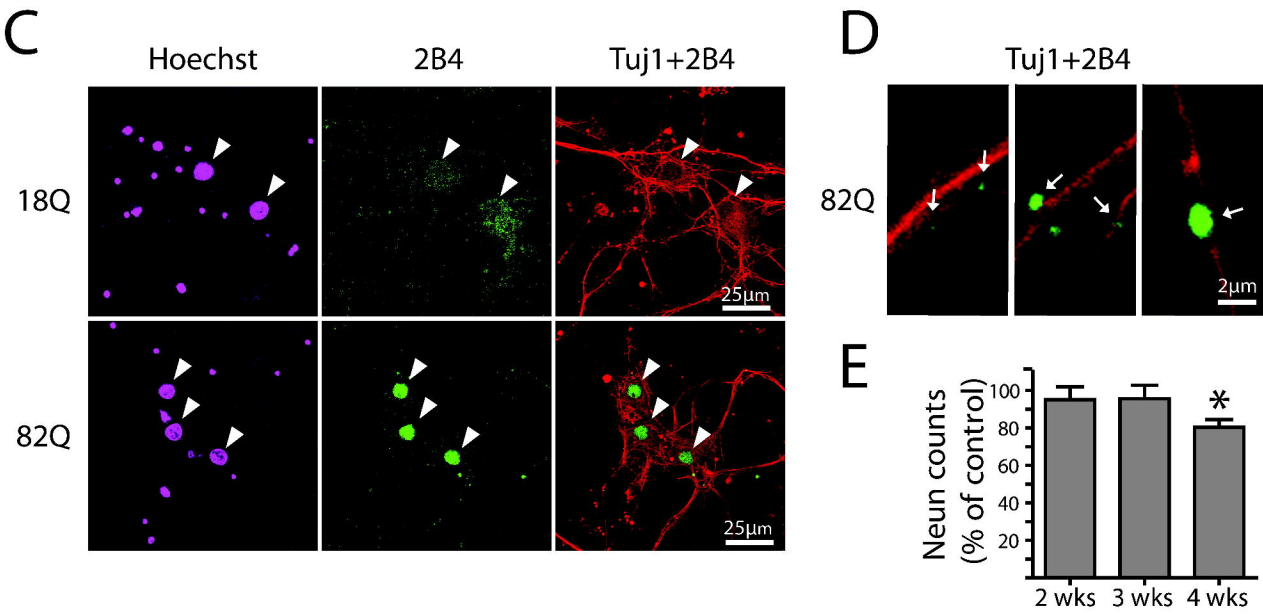
C
Hoechst
2B4
Tuj1+2B4
18Q
82Q
25µm
25µm
D
Tuj1+2B4
82Q
2µm
E
Neun counts (% of control)
100
80
60
40
20
*
2 wks
3 wks
4 wks

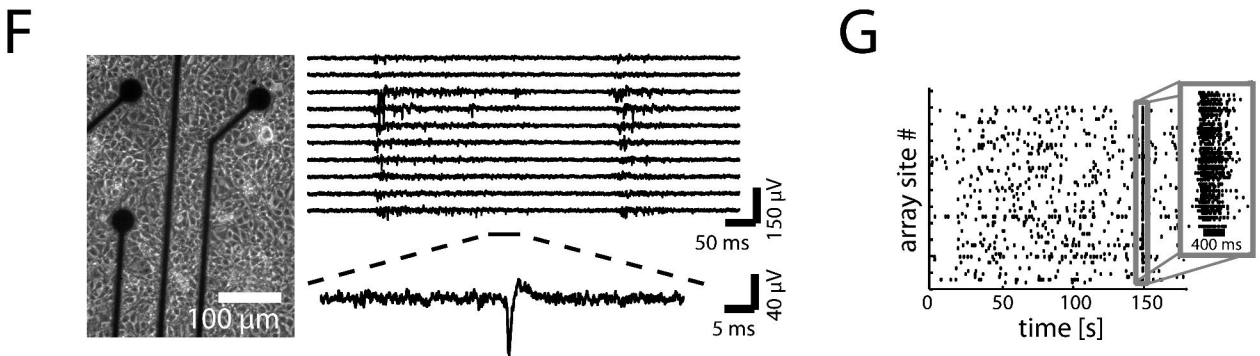
F
100 µm
150 µV
50 ms
40 µV
5 ms
G
array site #
0
50
100
150
time [s]
400 ms

Figure 2

JPET Fast Forward. Published on July 12, 2010 as DOI: 10.1124/jpet.
This article has not been copyedited and formatted. The final version may diff

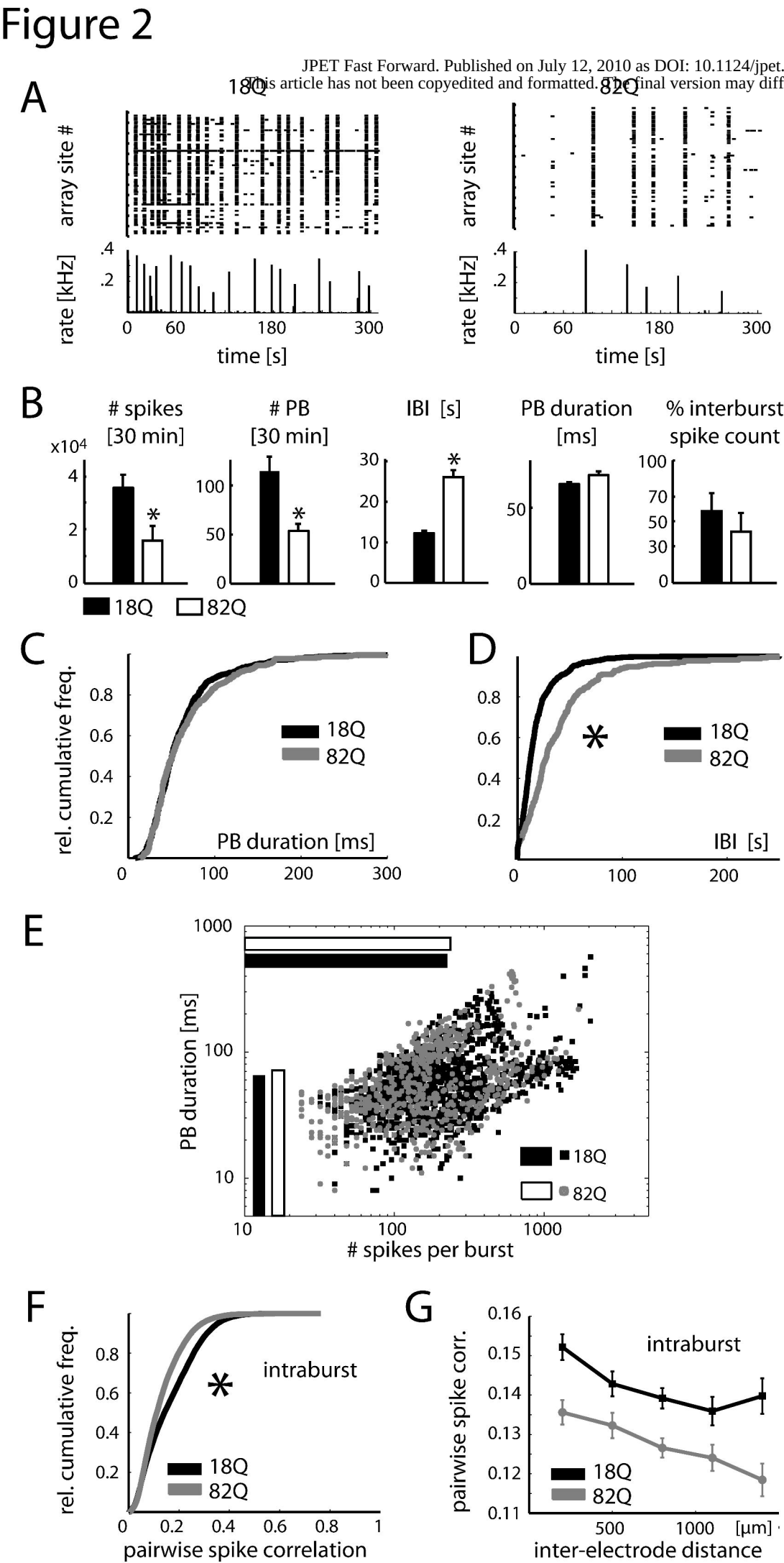

Figure 3

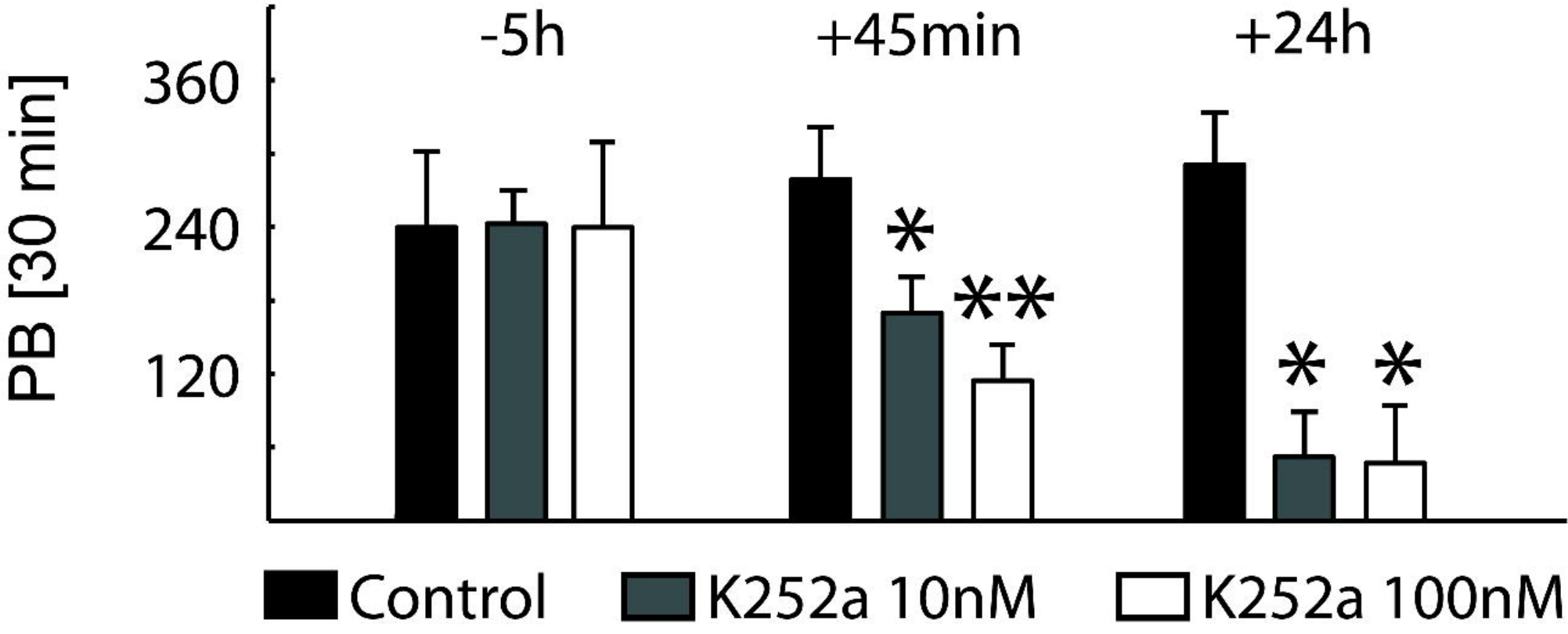
-5h
+45min
+24h
360
240
120
PB [30 min]
*
**
*
*
Control
K252a 10nM
K252a 100nM

Figure 4

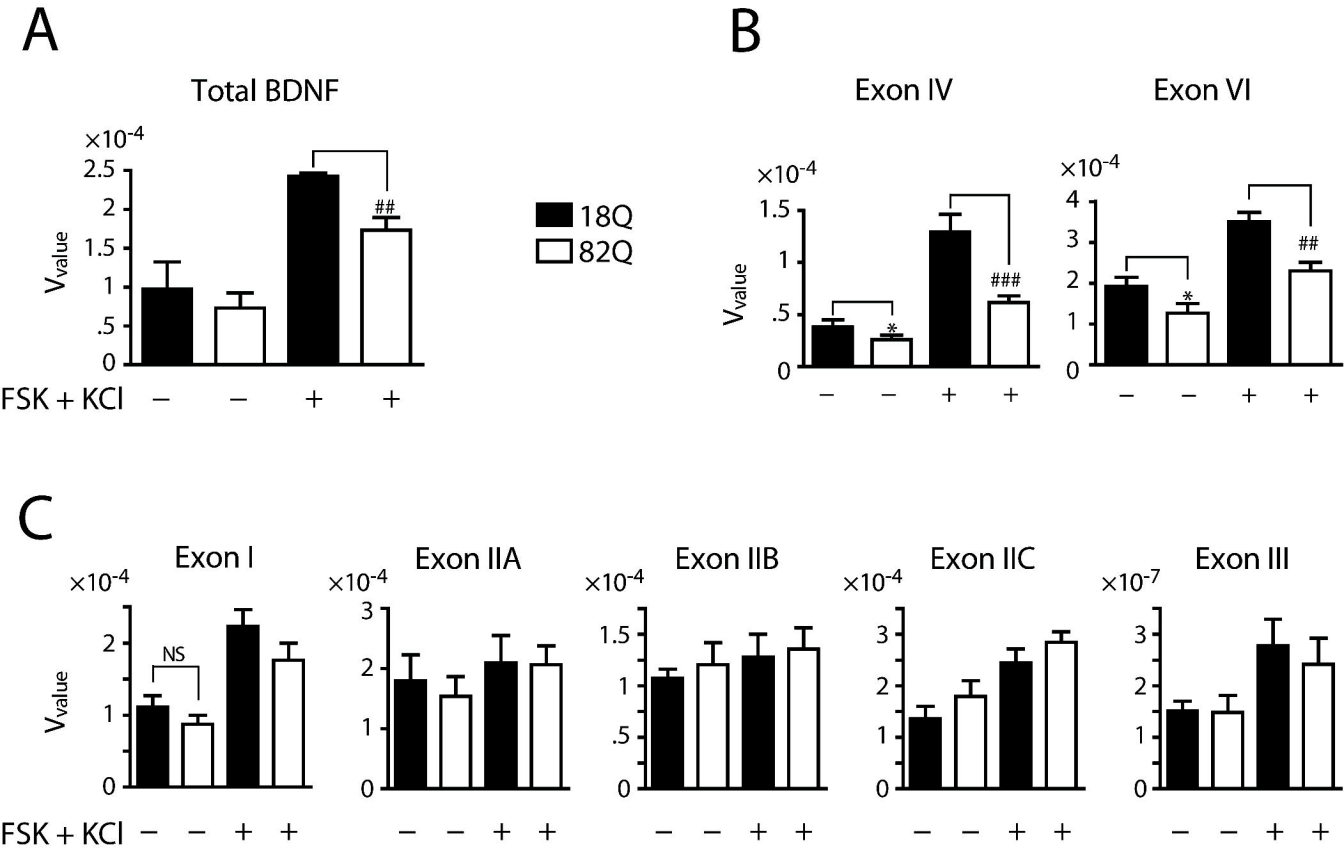
A
Total BDNF
×10-4
2.5
2
1.5
1
.5
0
Vvalue
##
18Q
82Q
FSK + KCl – – + +
B
Exon IV
×10-4
1.5
1
.5
0
Vvalue
*
###
– – + +
Exon VI
×10-4
4
3
2
1
0
*
##
– – + +
C
Exon I
×10-4
2
1
0
Vvalue
NS
FSK + KCl – – + +
Exon IIA
×10-4
3
2
1
0
– – + +
Exon IIB
×10-4
1.5
1
.5
0
– – + +
Exon IIC
×10-4
3
2
1
0
– – + +
Exon III
×10-7
3
2
1
0
– – + +

Figure 5

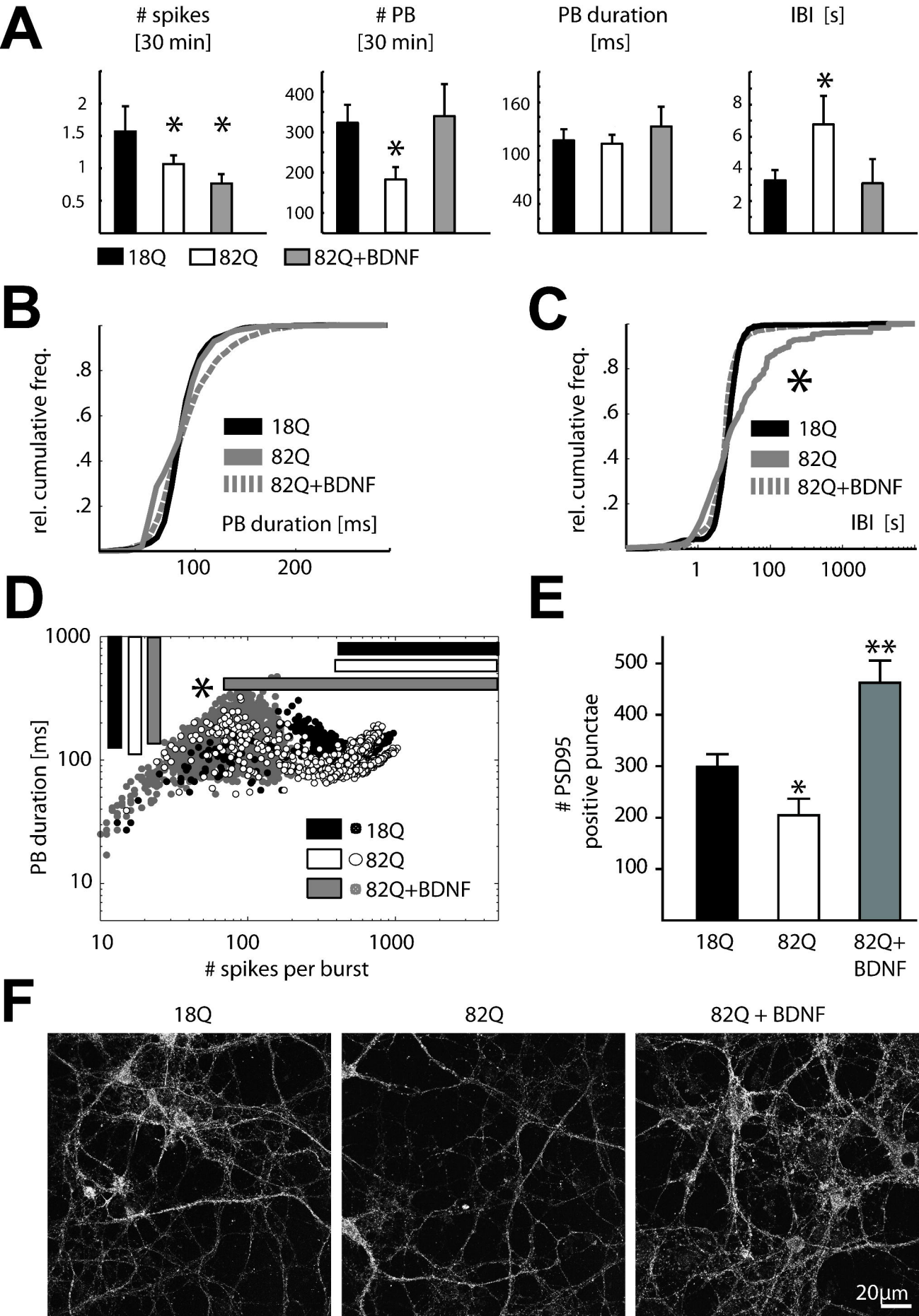
A
spikes [30 min]
PB [30 min]
PB duration [ms]
IBI [s]
18Q
82Q
82Q+BDNF
B
rel. cumulative freq.
PB duration [ms]
C
IBI [s]
D
PB duration [ms]
spikes per burst
E
PSD95 positive punctae
F
18Q
82Q
82Q + BDNF
20µm